

RESEARCH ARTICLE

Is human Achilles tendon deformation greater in regions where cross-sectional area is smaller?

Neil D. Reeves^{1,*} and Glen Cooper²**ABSTRACT**

The Achilles is a long tendon varying in cross-sectional area (CSA) considerably along its length. For the same force, a smaller CSA would experience higher tendon stress and we hypothesised that these areas would therefore undergo larger transverse deformations. A novel magnetic resonance imaging-based approach was implemented to quantify changes in tendon CSA from rest along the length of the Achilles tendon under load conditions corresponding to 10%, 20% and 30% of isometric plantar flexor maximum voluntary contraction (MVC). Reductions in tendon CSA occurring during contraction from the resting condition were assumed to be proportional to the longitudinal elongations within those regions (Poisson's ratio). Rather than tendon regions of smallest CSA undergoing the greatest deformations, the outcome was region specific, with the proximal (gastrocnemius) tendon portion showing larger transverse deformations upon loading compared with the distal portion of the Achilles ($P < 0.01$). Transverse tendon deformation only occurred in selected regions of the distal Achilles tendon at 20% and 30% of MVC, but in contrast occurred throughout the proximal portion of the Achilles at all contraction levels (10%, 20% and 30% of MVC; $P < 0.01$). Calculations showed that force on the proximal tendon portion was ~60% lower, stress ~70% lower, stiffness ~30% lower and Poisson's ratio 6-fold higher compared with those for the distal portion of the Achilles tendon. These marked regional differences in mechanical properties may allow the proximal portion to function as a mechanical buffer to protect the stiffer, more highly stressed, distal portion of the Achilles tendon from injury.

KEY WORDS: Magnetic resonance imaging, Gastrocnemius, Modulus, Stiffness, Injury

INTRODUCTION

The technique for testing human tendon mechanical properties *in vivo* has developed over the last ~15 years based upon the general principles of tendon tensile tests conducted *in vitro* (Butler et al., 1978; Cuming et al., 1978; Rigby, 1964). *In vivo* approaches have typically involved measuring longitudinal tendon elongations during isometric contraction using ultrasound imaging and relating these elongations to tendon force estimations derived from dynamometry measurements of joint torque (Maganaris and Paul, 1999). A necessary simplification with this approach is the measurement of

tendon elongations from a single anatomical point. Typically for 'free' tendons, this measurement point is the myo-tendinous junction (MTJ), or an osteo-tendinous interface, as these are clear 'reference' points that can be identified and tracked with ultrasound imaging. Intra-muscular tendon–aponeurosis sites have also been used for tracking tendon elongation at the site where fascicles intersect the aponeurosis. Although likely to be an oversimplification, the use of a single 'reference' point is a necessary step in obtaining measurements to permit calculation of tendon stiffness and modulus, with many current variations on the *in vivo* approach. It also allows specific questions to be answered relating to the variations in tendon properties between different populations (Hansen et al., 2003; Karamanidis and Arampatzis, 2006; Maganaris et al., 2006), or changes in tendon properties as a result of interventions (Arampatzis et al., 2007; Kubo et al., 2002; Reeves et al., 2005; Wiesinger et al., 2015). However, the implicit assumption with this approach is that tendon elongations are homogeneous, or at least representative of the entire tendon, which may not always be the case.

For relatively long tendons, *in vitro* studies have shown that variations in elongation occur along the length of the tendon (Wren et al., 2001; Zernicke et al., 1984). *In vivo* measurements also confirm the non-uniformity of tendon elongations along the length of the free tendon or tendon–aponeurosis in the human lower limb (Finni et al., 2003; Maganaris and Paul, 2000; Magnusson et al., 2003). Using an ultrasound speckle tracking approach, the human Achilles tendon has been shown to have differences in elongation between superficial and deeper regions (Arndt et al., 2012; Slane and Thelen, 2015). It might be hypothesised that elongation inhomogeneities should be particularly evident in long tendons where the cross-sectional area (CSA) varies considerably along the tendon length. This is because regions of the tendon with smaller CSAs are expected to experience higher stress (stress=force/area) and therefore are likely to experience greater transverse and longitudinal elongations. The CSA of the Achilles tendon varies considerably along its length (Finni et al., 2003; Magnusson and Kjaer, 2003), and we might hypothesise that because of this, the tendon will experience different elongations along its length, with smaller CSA regions experiencing larger transverse and longitudinal elongations.

The Achilles tendon is composed of two tendon components, with the more proximal gastrocnemius tendon 'fusing' with the soleus tendon just distal to the soleus muscle (Cummins and Anson, 1946). The 'fusing' of these two tendon components in a spiral manner (Cummins and Anson, 1946) also highlights the potential for shear to occur within the Achilles tendon, which may further contribute to non-uniform elongations along its length and in part explain changes seen with speckle tracking (Arndt et al., 2012; Slane and Thelen, 2015) and other ultrasound-based approaches (Bojsen-Moller et al., 2004; Magnusson et al., 2003). Larger elongations occurring at certain regions along the tendon may indicate a propensity for tendon strain injuries. If these regions coincide with portions of the tendon where the CSA is smaller, this may facilitate understanding of the

¹School of Healthcare Science, Faculty of Science & Engineering, Manchester Metropolitan University, John Dalton Building, Oxford Road, Manchester M1 5GD, UK. ²School of Mechanical, Aerospace & Civil Engineering, University of Manchester, Manchester M13 9PL, UK.

*Author for correspondence (N.Reeves@mmu.ac.uk)

 N.D.R., 0000-0001-9213-4580

List of symbols and abbreviations

A_o	average unloaded tendon section cross-sectional area (cm ²)
A_{ave}	average loaded tendon section cross-sectional area (cm ²)
CSA	cross-sectional area (cm ²)
E	average Young's modulus of tendon section (MPa)
EMG	electromyographic
F	force on the tendon section (N)
K	average stiffness of tendon section (N mm ⁻¹)
L_o	original tendon section length (mm)
MRI	magnetic resonance imaging
MTJ	myo-tendinous junction
MVC	maximal voluntary contraction
PCSA	physiological cross-sectional area
V_o	original volume of tendon section
ΔL	change in tendon section length (mm)
ΔV	change in volume of tendon section
Δx	extension of tendon section
ϵ_x	average strain of tendon section
ν	Poisson's ratio for tendon section
σ	average engineering stress in tendon section (MPa)

mechanisms of tendon injuries and ruptures. The most frequent site (in 85% of cases) for complete rupture of the Achilles tendon is reported to be the region 3–5 cm proximal to the calcaneus (Józsa et al., 1989). This also coincides with the region of the Achilles tendon where the CSA is at its smallest (Magnusson and Kjaer, 2003), supporting the hypothesis for a link between regions of higher stress, greater transverse/longitudinal elongations and propensity for tendon injury.

As current conventional *in vivo* techniques cannot distinguish transverse length-dependent deformations, we adopted a novel magnetic resonance imaging (MRI)-based approach to assess tendon deformation occurring along the length of the Achilles tendon, with the hypothesis that larger transverse deformation would be observed at regions of the tendon where the CSA is smaller. This experimental approach involved measuring tendon CSA changes in the transverse plane with the assumption that tensile loading causes a reduction in CSA proportional to the longitudinal elongation (Poisson's ratio); essentially, as the tendon is stretched it becomes proportionally thinner.

MATERIALS AND METHODS**Participants**

Nine male participants (mean±s.d. age: 25±6 years, body mass: 80±10 kg and height: 1.81±0.05 m) gave informed consent to take part, after the study had received institutional ethics committee approval. Exclusion criteria included: contraindication to MRI scanning, prior lower limb surgery, tendinopathy affecting the Achilles or tendons of the lower limbs, and serious injury to the Achilles tendon or lower limb.

Determining the statistical power with the results obtained tested the adequacy of the sample size against the optimal of 80% power recommended by Cohen (1988). In the proximal (gastrocnemius) tendon region, statistical power was 100% and ranged between 40–79% in the region of smallest CSA.

Dynamometry

Participants lay prone on the chair of an isokinetic dynamometer (Cybex Norm, NY, USA) with the right foot fixed into the footplate at a neutral ankle position [i.e. 1.57 rad (90 deg) between foot plate and tibia] and the knee in full extension. Participants first performed isometric maximal voluntary contraction (MVC) of the plantar flexors on the dynamometer. Two isometric MVCs were performed (an additional contraction was performed if the two MVC torque values

were not within 5% of each other) and the mean torque value was calculated. Joint torque values corresponding to 10%, 20% and 30% of a participant's MVC were then calculated and visually highlighted on a screen for the participant, displaying the torque trace in real time, linked to an acquisition system (Biopac Systems Inc., CA, USA). Using visual feedback, participants were then asked to perform a plantarflexion contraction, developing the torque value corresponding to 10%, 20% and 30% of their MVC (in a randomised order) and maintain this value for 3 min at each percentage of their MVC (with 3 min rest between MVC levels). Simultaneously during these plantarflexion contractions, electromyographic (EMG) activity was measured from the tibialis anterior muscle to assess the level of co-contraction (see 'Antagonist muscle co-contraction', below) and the MTJ of the gastrocnemius muscle–tendon unit was tracked using B-mode ultrasound imaging to assess tendon elongation (see 'Measurement of tendon elongation and assessment of tendon creep', below).

Antagonist muscle co-contraction

To estimate the level of dorsiflexor co-activation during plantarflexion efforts, the EMG activity was measured from a representative dorsiflexor muscle (tibialis anterior). The root mean square EMG activity was calculated from the raw signal and related to that measured from the same muscle (tibialis anterior) when acting as an agonist during dorsiflexion contractions at various percentages of the dorsiflexion MVC. The level of dorsiflexor co-activation and the corresponding co-activation torque during plantarflexion efforts at 10%, 20% and 30% of MVC were then calculated in line with previously described methods (Maganaris et al., 1998b).

Measurement of longitudinal tendon elongation and assessment of tendon creep

During dynamometry testing, the medial head of the gastrocnemius MTJ was scanned at 25 Hz using ultrasound imaging (Mylab 70, Esaote, Italy), in line with previously described methods (Maganaris and Paul, 2002; Reeves et al., 2005), to represent the longitudinal elongations of the whole Achilles tendon. It was previously reported that there are no significant differences in Achilles tendon stiffness and strain between scanning at the MTJ of the medial or lateral head of the gastrocnemius (Morrison et al., 2015). The ultrasound probe was secured in position using a custom-made holder to prevent any movement relative to the scanned structure, and an external marker placed onto the skin casting a line on the image and confirming that no movement took place. The longitudinal displacement of the gastrocnemius MTJ was tracked continuously during the 3 min plantarflexion contraction performed at each contraction level (10%, 20% and 30% of MVC). Scans were then digitised offline using Image J (National Institutes of Health, Bethesda, MD, USA) at 1 min intervals (i.e. tendon elongation was measured at 0, 1, 2 and 3 min time intervals). These scans were acquired to assess the degree of overall longitudinal Achilles tendon elongation and to identify whether any tendon creep was evident during these sustained contractions.

MRI scanning

Participants were positioned supine, with the knees fully extended within a 0.25 T MRI scanner (G-Scan, Esaote, Italy). Axial plane scans of participant's right lower leg were acquired using a Spin-Echo Fast Fourier sequence with the following scanning parameters: 1:59 min scanning time, 18 ms echo time, 1020 ms repetition time, 1 acquisition, 180×170 mm field of view, 256×256 pixels, 7 mm slice thickness, 1 mm inter-slice gap. These scans were acquired (foot fixed in the neutral position) with the participant at rest and also while developing an isometric plantarflexion contraction (with the knee

fully extended), with a torque equivalent to 10%, 20% and 30% of their MVC (determined from the dynamometry measurements described above). Development of these prescribed isometric joint torque levels (10%, 20% and 30% of MVC) was achieved by using a custom-made, MRI-compatible lever system. The participant's external lever arm (defined as the distance from the ankle joint centre of rotation to the point of force application at the first metatarsal head) and the device lever arm were carefully measured using a ruler incremented in millimetres. Loads that would achieve the required plantarflexion torque levels were then calculated and positioned on one end of the lever system. The other end of the lever system was in contact with the participant's foot (the first metatarsal head region), where the application of force acted to secure the system in place around a pivot point on the MRI bed. When the scan began, an experimenter positioned inside the MRI released the load. Participants then needed to develop a plantarflexion joint torque (isometric contraction) equivalent to the prescribed level that would balance the load within a small, tightly controlled range, verified visually by the experimenter. This process was repeated for each level of joint torque (10%, 20% and 30% of MVC). Axial plane scans were acquired starting from the calcaneus and continuing ~17 cm proximal from this point, capturing the entire length of the distal portion of the Achilles tendon and the vast majority of the proximal (gastrocnemius) tendon portion (Fig. 1). Moving proximally from the calcaneus, the first appearance of the Achilles tendon was designated as 'scan 0'. Using digitising software (OsiriX, Pixmeo, Geneva, Switzerland), the CSA of the Achilles tendon was then measured on scans 2–21 (Figs 1 and 2). The distal portion of the Achilles tendon was defined as that composed of both soleus and gastrocnemius tendons. Moving proximally from the calcaneus, the first appearance of the soleus muscle (i.e. the soleus MTJ) therefore delineated where the distal portion of the Achilles tendon ended and the proximal portion (gastrocnemius) of the Achilles tendon began (Fig. 1).

Sagittal plane MRI scans were acquired for the purpose of quantifying the Achilles tendon moment arm length, which was used for calculating tendon force by dividing the measured plantarflexion joint torque by the Achilles tendon moment arm length. Scans were taken with the foot in the neutral ankle position, in 0.17 rad (10 deg) of dorsiflexion and 0.17 rad (10 deg) of plantarflexion. During the scans, participants were asked to perform a plantarflexion contraction to the level of ~20% MVC so that the Achilles tendon moment arm was measured under load, because the Achilles tendon moment arm is known to increase when a tensile load is applied compared with the resting state (Maganaris et al., 1998a). The Achilles tendon moment arm length was calculated for a neutral ankle position using the Reuleux method as previously described in detail (Maganaris et al., 1998a). Briefly, scans taken in dorsiflexion and plantarflexion were used to identify the instant centre of rotation on the talus bone in the neutral ankle scan. The Achilles tendon moment arm length was then measured as the perpendicular distance between the Achilles tendon action line and the joint centre of rotation on the talus in the neutral ankle scan.

Estimation of mechanical properties of the Achilles tendon proximal and distal components

Mechanical and material properties were calculated separately for the distal and proximal portions of the Achilles tendon as described below. Overall Achilles tendon length was estimated using the participant's height and multiplying by a factor of 0.00792 (calculated from tendon data from Reeves et al., 2005). MRI scans were used to measure the length of the distal portion of the Achilles tendon by summing the number of slices from the calcaneus insertion to the

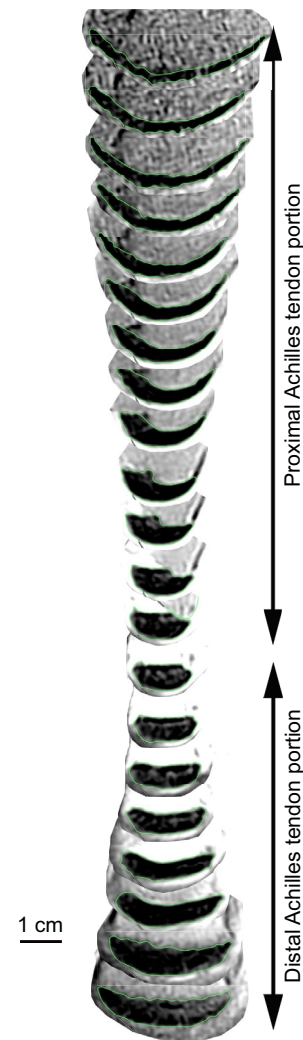


Fig. 1. Example series of axial plane magnetic resonance imaging (MRI) scans showing tendon cross-sectional areas (CSA) measured in one participant. The tendon CSAs are delineated by the green line. The first appearance of the soleus muscle can be seen, which defined where the proximal component of the Achilles tendon began.

soleus MTJ (7 mm slice thickness+1 mm gap=8 mm resolution). The length of the proximal portion of the Achilles tendon was estimated by subtracting the length of the distal portion from the overall Achilles tendon length. The overall longitudinal tendon elongation was measured using ultrasound at the gastrocnemius medial MTJ and longitudinal elongation for each section, ΔL , was estimated by assuming that elongation at the soleus MTJ was 30% less than elongation of the overall Achilles tendon (Bojsen-Moller et al., 2004).

Mechanical stiffness, K , for both proximal and distal components of the Achilles tendon was estimated by dividing force applied, F , by the extension, Δx (Eqn 1), on the respective tendon components:

$$K = \frac{F}{\Delta x}. \quad (1)$$

During *in vitro* testing taken until failure, the tendon longitudinal force–elongation behaviour can be observed to move from a ‘toe’ region into a well-defined ‘linear’ elongation region. During *in vivo* tendon mechanical tests, although the tendon longitudinal force–elongation behaviour may begin to enter into a linear region following on from the curvilinear toe region, any linear region is not as well defined as that during *in vitro* tests. The approach to

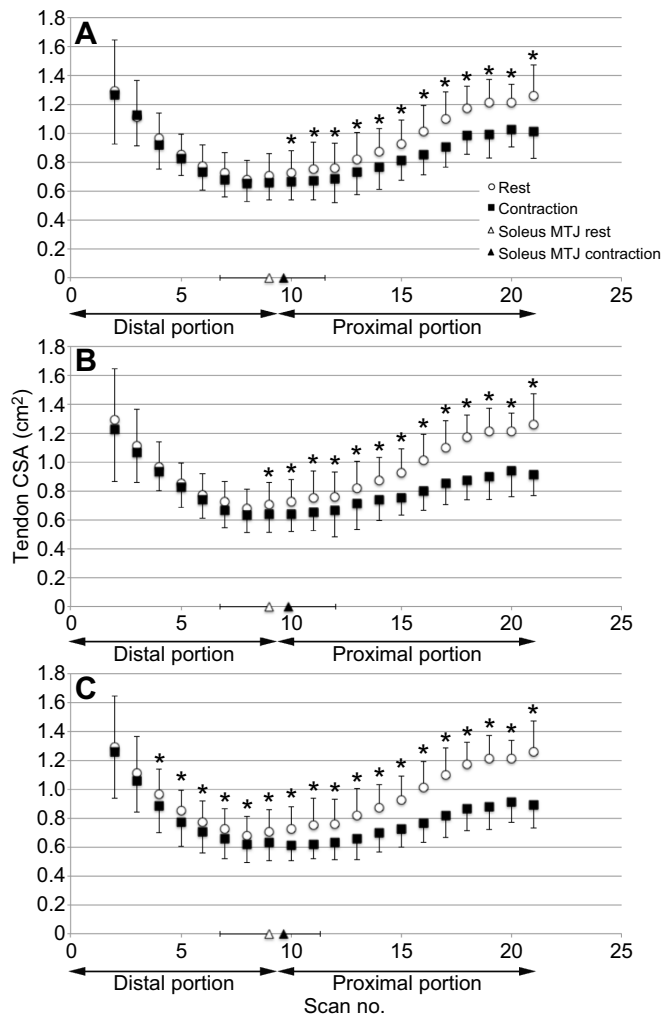


Fig. 2. CSA along the length of the Achilles tendon at rest and during isometric contraction. Isometric contraction was maintained at defined contraction levels of (A) 10%, (B) 20% and (C) 30% of plantarflexion maximum voluntary contraction (MVC). *Significantly ($P < 0.01$) different from rest. MTJ, myo-tendinous junction. Scan 0 is the first appearance of the Achilles tendon above the calcaneus. Data are means and s.d. ($n=9$).

calculating tendon stiffness *in vivo* therefore typically relies upon assuming linearity of the tendon's force–elongation curve over small, well-defined regions of this curve (Maganaris and Paul, 1999). The tendon force–elongation curve was therefore assumed to be linear over the small force regions where it was measured, i.e. 0–10%, 10–20% and 20–30% MVC.

Young's modulus, E , was calculated separately for the distal and proximal tendon regions by taking the average resting CSA from each of the tendon sections, A_o , and calculating the average stress, σ , and the average strain, ϵ_x (where L_o is the original tendon section resting length), in the longitudinal direction (Eqns 2–5):

$$A_o = \sum_{i=1}^n \frac{A_i}{n}, \quad (2)$$

$$\sigma = \frac{F}{A_o}, \quad (3)$$

$$\epsilon_x = \frac{\Delta x}{L_o}, \quad (4)$$

$$E = \frac{\sigma}{\epsilon}. \quad (5)$$

Poisson's ratio, ν , was calculated from the tendon volume change, ΔV , and the original tendon volume, V_o , using Eqn 6. Tendon volume was calculated using MRI measurements. The distal Achilles tendon portion was measured in full but only ~70% of the proximal (gastrocnemius) component of the Achilles tendon was directly measured by the MRI, so a subject-specific multiplying factor was used to calculate total volume (Reeves et al., 2005):

$$\nu = \frac{1}{2} - \frac{\Delta V}{2 V_o \epsilon_x}. \quad (6)$$

Load sharing between the Achilles tendon components was estimated as 59% of the plantar flexor joint moment for the distal component of the Achilles tendon and 24% for the proximal component of the Achilles tendon based upon muscle physiological cross-sectional area (PCSA) data (Fukunaga et al., 1992). Other plantar flexor muscles (tibialis posterior, flexor hallucis longus and flexor digitorum longus) were assumed to carry the remaining 17% of the load (peroneus longus and brevis muscles were not included as their main role was assumed to be ankle eversion and, furthermore, there were no PCSA data available for these muscles relative to the other plantar flexors).

Statistical analysis

A repeated measures analysis of variance (ANOVA) with a Newman–Keuls multiple comparison *post hoc* test was applied to test for differences between contraction conditions (rest, 10%, 20% and 30% MVC). This statistical approach was used for the parameters of tendon CSA, tendon longitudinal elongation, plantar flexor joint torque and dorsiflexor muscle co-activation. A paired samples Student's *t*-test was used to test for differences in mechanical properties between the distal and proximal portions of the Achilles tendon. Values presented are means \pm s.d.

RESULTS

Regional Achilles tendon CSA changes upon loading

At 10% of MVC, CSAs were significantly smaller throughout the proximal Achilles tendon component compared with those at rest ($P < 0.01$), but there was no significant difference in the distal Achilles tendon CSAs (Fig. 2A). At 20% and 30% of MVC, CSAs throughout the proximal Achilles tendon component remained significantly smaller compared with those at rest ($P < 0.01$; Fig. 2B,C). At 20% of MVC, the most superior CSA of the distal Achilles tendon component (scan 9) was significantly smaller compared with that at rest ($P < 0.01$), with no significant difference in any other CSAs throughout the distal Achilles tendon component (Fig. 2B). At 30% of MVC, CSAs in the superior region of the distal Achilles tendon (scans 4–9) were significantly smaller compared with those at rest ($P < 0.01$; Fig. 2C), with no significant difference at the most inferior CSAs of the distal Achilles tendon component (scans 2 and 3).

Longitudinal Achilles tendon elongations

Longitudinal elongations of the whole Achilles tendon measured using ultrasound are shown in Fig. 3 (see below). Elongations of the whole Achilles tendon measured at 0, 1, 2 and 3 min during the sustained isometric contractions were not significantly different between any of these time points, for any of the contraction levels (Fig. 3).

Plantarflexion joint torque and Achilles tendon moment arm

Table 1 shows how participants were able to be very accurate with matching the target plantarflexion torque over the duration of

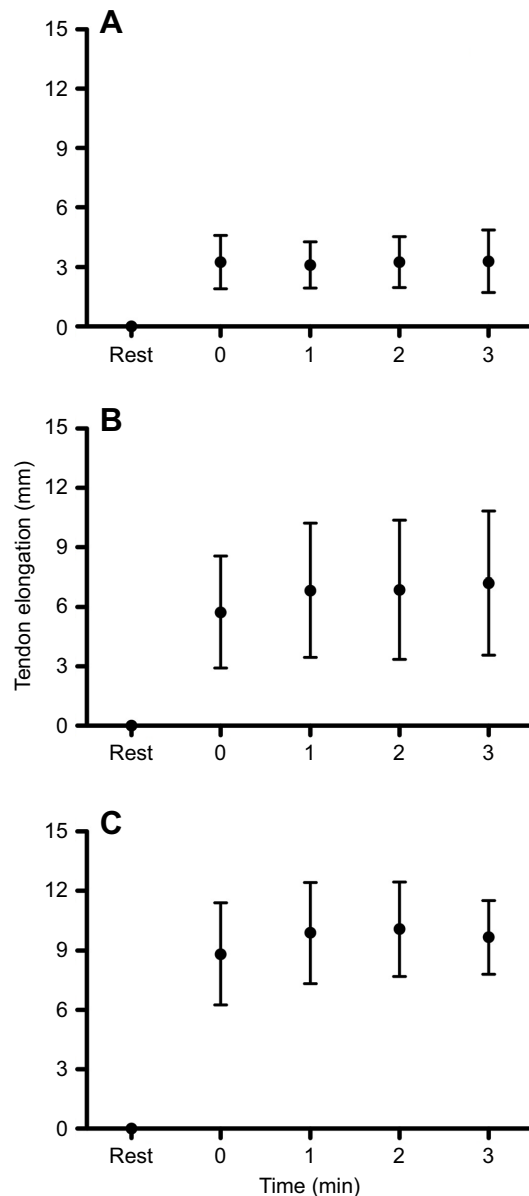


Fig. 3. Longitudinal elongation of the Achilles tendon measured at the medial gastrocnemius MTJ using ultrasound at rest and during isometric contraction. Isometric contraction was maintained at defined contraction levels of (A) 10%, (B) 20% and (C) 30% of plantarflexion MVC for up to 3 min, with measurements being taken immediately upon contraction (time 0 on the x-axis) and subsequently every minute. Data are means \pm s.d. ($n=9$).

the 3 min contraction on the dynamometer, with little variation around the mean. Table 2 shows the Achilles tendon moment arm lengths for each individual participant as well as the group mean and s.d.

Dorsiflexor co-activation

The level of dorsiflexor coactivation during plantar flexor efforts was $<1\%$ expressed as a proportion of the maximum agonist dorsiflexor EMG and <1 N m when the torque contribution from this level of co-activation was calculated. There were no significant differences in co-activation between contraction levels (% MVC) or over time during the sustained isometric contraction.

Mechanical properties of the distal and proximal components of the Achilles tendon

Table 3 shows the mechanical properties for the distal and proximal components of the Achilles tendon at the three different loading levels (10%, 20% and 30% MVC). The proximal component of the Achilles tendon was significantly longer (L_0), experienced $\sim 60\%$ lower force (F), $\sim 70\%$ lower stress (σ), $\sim 30\%$ lower stiffness (K) and 6-fold higher Poisson's ratio (ν) compared with the distal Achilles tendon component (Table 3).

DISCUSSION

In this study, we adopted a novel MRI-based approach to study transverse tendon deformations occurring throughout the length of the Achilles tendon, with the initial hypothesis that deformation would be greater where tendon CSA is smaller. This experimental approach involved measuring tendon CSA changes in the transverse plane with the assumption that tensile loading causes a reduction in CSA proportional to the longitudinal elongation (Poisson's ratio); essentially, as the tendon is stretched it becomes proportionally thinner. Our initial hypothesis, that the tendon would undergo larger deformations in regions of smaller CSA, was based upon the assumption that material properties and forces were similar throughout the tendon's length. Therefore, areas where the tendon CSA was smaller would experience higher stress and undergo larger transverse and longitudinal deformations. The present results do not support this hypothesis, but instead support the intriguing notion that Achilles tendon deformation is region specific and closely related to differences in mechanical properties between the proximal (gastrocnemius) and distal components of the Achilles tendon (Figs 1 and 2, Table 3).

In the present study, we applied tensile loading via isometric muscle contraction at 10%, 20% and 30% of MVC. At 10% of MVC, we found reductions in CSA throughout the length of the proximal (gastrocnemius) Achilles tendon portion, but no changes in the distal portion of the Achilles tendon (Fig. 2A). Selected superior regions of the distal portion of the Achilles tendon only began to show reductions in CSA upon loading at 20% and 30% of MVC, with no changes to inferior regions of the distal tendon portion (Fig. 2B,C). These results show that rather than the region of smallest tendon CSA undergoing larger transverse deformations due to tensile loading, there is a marked difference between proximal and distal regions of the Achilles tendon. Specifically, in the proximal region of the Achilles tendon, force was $\sim 60\%$ lower, stress was $\sim 70\%$ lower, stiffness was $\sim 30\%$ lower and Poisson's ratio was 6-fold higher compared with the distal portion of the Achilles tendon (Fig. 2, Table 3). Substantially greater transverse strain in the proximal compared with the distal region of the Achilles tendon explains the 6-fold higher Poisson's ratio value for this proximal Achilles tendon region.

The substantially lower forces acting on the proximal portion of the Achilles tendon ($\sim 60\%$ lower) can be explained because only forces generated proximal to the gastrocnemius MTJ by the gastrocnemius muscle act to deform this proximal Achilles tendon region. In contrast, the more distal portion of the Achilles tendon experiences much higher forces generated by both proximally located muscles: the gastrocnemius and soleus (Table 3). Substantially lower forces in the proximal Achilles tendon region contribute to explaining the markedly lower stiffness ($\sim 30\%$ lower) compared with the distal tendon portion (Table 3). The lower stiffness of the proximal Achilles tendon region may allow it to function as a 'buffer', absorbing high strains induced by high force eccentric contractions and thereby protecting the stiffer, more highly

Table 1. Joint torque during plantarflexion contractions at 10%, 20% and 30% of maximal voluntary contraction (MVC)

Target	Torque (N m)								
	10% MVC			20% MVC			30% MVC		
	Actual	s.d.	Target	Actual	s.d.	Target	Actual	s.d.	
12.3±3.4	12.3±3.4	0.3±0.1	24.6±6.8	24.5±6.7	0.4±0.2	36.9±10.2	36.5±10	0.6±0.3	

Values are means±s.d. for the target torque, the actual torque (mean over 3 min duration) and s.d. (the variance around the mean over the 3 min duration).

stressed, distal portion of the Achilles tendon. The capacity of the tendon to act as a buffer and protect the muscle fascicles from injury by attenuating the force and slowing the rate of lengthening for muscle fascicles has previously been identified (Konow and Roberts, 2015; Konow et al., 2012; Roberts and Konow, 2013). We speculate that the proximal portion of the Achilles tendon may function as a buffer not only to protect the muscle fascicles but also to protect the stiffer, more highly stressed, distal portion of the Achilles tendon.

A tendon's modulus reflects the intrinsic 'material' properties of the tendon and is given by the stiffness normalised to the dimensions of the tendon (Maganaris and Paul, 1999; Reeves et al., 2003). As the CSAs of these two tendon regions (proximal and distal Achilles tendon regions) are fairly equivalent (see Fig. 2 and Table 3) and our findings show the stiffness of the proximal tendon region to be lower, these results might indicate a lower modulus of the proximal Achilles tendon; however, this was not found to be the case (Table 3). The stiffness values in the present study ranged between 51 and 132 N mm⁻¹, which agrees well with a number of previously reported values for the Achilles tendon ranging between 26 and 187 N mm⁻¹ (Arampatzis et al., 2007; Karamanidis and Arampatzis, 2006; Kubo et al., 2002; Maganaris and Paul, 2002; Reeves et al., 2005), but is lower than some other reports for the same tendon, ranging between 486 and 2000 N mm⁻¹ (Couppe et al., 2016; Kongsgaard et al., 2011; Magnusson et al., 2003, 2001). These apparent discrepancies across the literature can probably be explained by a number of factors including the proportion of force attributed to the Achilles tendon from the measured joint torque, differing sections of the force–elongation curve examined and variance in the anatomical structures tracked to measure longitudinal elongations.

Consistent with our findings in the 'free' Achilles tendon, a greater elongation of the gastrocnemius compared with the soleus tendon–aponeurosis has been observed using ultrasound imaging during maximal and sub-maximal contractions with the knee in full extension (Bojsen-Moller et al., 2004). Through the insertion and tracking of a needle into the 'free' Achilles tendon, it has been reported that the elongation and strain of the free Achilles tendon (corresponding to the distal portion of the Achilles tendon in the

present study) was greater than an intra-muscular point tracked on the medial gastrocnemius tendon–aponeurosis (Magnusson et al., 2003). These previous findings are broadly in line with those of the present study when considering the two separate regions of the Achilles tendon; the present study found greater elongation and longitudinal strains in the distal Achilles tendon (equivalent to the 'free' tendon of the previous study) compared with the proximal Achilles tendon region (Table 3). Previous work using a 3D ultrasound approach found 3 mm elongation in the Achilles tendon and 3 mm elongation in the proximal gastrocnemius component of the Achilles tendon during contraction at 50% of MVC (Farris et al., 2013). Similar elongations between these two components of the Achilles tendon with markedly lower forces acting on the gastrocnemius tendon component are in line with our assertions of a lower stiffness for the proximal (gastrocnemius) compared with the distal Achilles tendon. Because of the greater length of the proximal Achilles tendon (gastrocnemius) compared with the distal region, these elongations correspond to smaller longitudinal strains in the proximal tendon component, consistent with MRI-based findings at 30% and 60% of MVC (Iwanuma et al., 2011). These previous reports, however, reflect overall 'end-to-end' length changes of these tendon components rather than more detailed region specificity as examined in the present study. An increased width measured at the gastrocnemius MTJ was noted upon contraction in a previous report (Farris et al., 2013). In another report, an increased width of the proximal (gastrocnemius) Achilles tendon component but a decreased width of the distal Achilles tendon component during contractions at 30% and 60% of MVC was noted (Iwanuma et al., 2011). Whilst girth measurements at a single site such as the MTJ may result from muscle bulging, tensile deformation of a tendon should only result in thinning of its overall CSA (Poisson's ratio) and therefore consideration of only one axis in the transverse plane may not reveal the true nature of deformation during tendon loading. In the present study, the 6-fold higher Poisson's ratio of the proximal compared with the distal Achilles tendon region reflects the substantial 'thinning' of the proximal tendon region during tensile loading.

We initially hypothesised that larger CSA reductions, inferring larger longitudinal elongations, would occur in areas where the tendon CSA was smaller. In sharp contrast, we found larger CSA reductions, inferring larger longitudinal elongations, in the proximal Achilles tendon region where tendon CSA was actually greatest (Fig. 2). This finding raises at least two main possibilities. (1) Forces may not be distributed equally throughout the length of the Achilles tendon and areas of smaller CSA may experience lower forces and stresses. (2) There may be differences in the Achilles tendon's material properties along its length that could result from changes in the volume fraction, with collagen fibre-to-matrix ratios increasing in areas where the tendon CSA is smaller.

Although possible, option 1 seems unlikely as the forces experienced in the smaller CSA regions would need to be substantially lower than those in other regions to compensate for the smaller CSA. Although not implausible, it is difficult to understand how the forces transmitted through an in-series structure

Table 2. Achilles tendon moment arm lengths

Participant	Moment arm length (mm)
1	48
2	49.5
3	49.2
4	54.9
5	57.7
6	44.8
7	38.6
8	64.4
9	51.5
Mean	50.9
s.d.	7.5

Individual values for each participant are shown, in addition to the group mean and s.d.

Table 3. Mechanical properties for the Achilles tendon components

Achilles tendon	Values	Property	10% MVC	20% MVC	30% MVC
Overall	Measured	A_o	0.95±0.14	0.95±0.14	0.95±0.14
		A_{ave}	0.84±0.16	0.83±0.16	0.80±0.15
		ΔL_{full}	2.7±0.9	6.7±2.2	10.1±2.2
		T	12.3±3.4	24.5±6.7	36.5±10.0
Proximal	Measured	A_o	0.95±0.14	0.95±0.14	0.95±0.14
		A_{ave}	0.84±0.16	0.83±0.16	0.80±0.15
		Calculated			
		F	65±16**	129±32**	193±47**
		L_o	147±11**	147±11**	147±11**
		ΔL	0.8±0.3**	2.0±0.7**	3.0±0.7**
		σ	0.7±0.1**	1.4±0.3**	2.0±0.4**
		ϵL	0.6±0.2**	1.4±0.5**	2.0±0.4**
		ϵT	-2.5±5.5	-6.2±8.0	-7.9±8.2
		K	89±27**	51±10**	86±37**
		E	125±50	101±32	95±21
		ν	6.4±10.8	3.8±6.1	3.7±3.7*
Distal	Measured	A_o	0.92±0.21	0.92±0.21	0.92±0.21
		A_{ave}	0.90±0.17	0.87±0.16	0.85±0.17
	Calculated	F	159±39	317±78	474±116
		L_o	81±11	81±11	81±11
		ΔL	1.9±0.7	4.7±1.6	7.1±1.5
		σ	2.5±0.9	5.0±1.7	7.5±2.6
		ϵL	2.4±0.9	5.8±2.2	9.2±2.5
		ϵT	-1.0±3.3	-2.4±4.1	-3.3±4.6
		K	132±40	75±15	128±55
		E	114±56	100±53	85±28
		ν	0.3±1.7	0.1±1.4	0.3±0.6

Moment arm length (r), 50.9±7.5 mm; participant height (h), 1.81±0.05 m. A_o , average unloaded tendon cross-sectional area (cm²); A_{ave} , average loaded tendon cross-sectional area (cm²); ΔL_{full} , overall change in full Achilles tendon length (mm); T , joint torque developed at the ankle (N m); F , force on the tendon section (N); L_o , original tendon section length (mm); ΔL , change in tendon section length (mm); σ , average engineering stress in tendon section (MPa); ϵL , average longitudinal strain in tendon section (%); ϵT , average transverse strain in tendon section (%); K , average stiffness of tendon section (N mm⁻¹); E , average Young's modulus of tendon section (MPa); ν , Poisson's ratio for tendon section.

Values are means±s.d. Asterisks denote significant differences from the distal component of the Achilles tendon (* P <0.05 and ** P <0.01).

could vary so drastically. The density and area fraction of collagen fibrils have been shown to vary between different regions of the rabbit patellar tendon (Williams et al., 2008), raising the possibility that changes to the collagen fibre-to-matrix ratio (option 2) may occur along the length of the human Achilles tendon. If this collagen fibre-to-matrix ratio increases in regions of smaller tendon CSA, it may increase the modulus in these Achilles tendon regions and contribute towards explaining the current findings.

The finding of differential deformations along the length of the proximal and distal Achilles tendon components is in line with previous *in vivo* reports of non-uniform longitudinal elongations in the soleus tendon–aponeurosis and tibialis anterior muscle–tendon unit (Finni et al., 2003; Maganaris and Paul, 2000). Differences in elongation have also been reported between the gastrocnemius tendon–aponeurosis and the Achilles tendon (Bojsen-Moller et al., 2004; Magnusson et al., 2003). Our findings are also in line with *in vitro* reports of non-uniform elongations along the length of the human Achilles and other long tendons (Wren et al., 2001; Zernicke et al., 1984). As the gastrocnemius and soleus tendons ‘fuse’ to form the Achilles tendon distal to the soleus muscle, there is the potential for intra-tendinous shear to occur within the Achilles tendon. Indeed, the propensity for shear within the Achilles tendon has been indicated from *in vivo* (Bojsen-Moller et al., 2004; Magnusson et al., 2003) and *in vitro* (Lersch et al., 2012) human studies.

Three muscles (gastrocnemius medial and lateral heads and soleus) generate force applied to the Achilles tendon and their individual force contributions will vary according to their PCSA (Fukunaga et al., 1992). These three muscles may also be activated to different relative levels at any given joint torque. Indeed, activation of the lateral gastrocnemius muscle was shown to be

relatively low at 30% of maximum voluntary plantarflexion contraction compared with that of the medial gastrocnemius (Masood et al., 2014). This highlights the complexity of loading on the Achilles tendon with contributions from three independent muscles, which have been suggested to constitute mechanically separate tendon compartments within the Achilles (Bojsen-Moller and Magnusson, 2015). Indeed, ultrasound speckle tracking methods have shown greater elongation within the deeper region of the Achilles tendon compared with the superficial layer during loading (Arndt et al., 2012; Franz et al., 2015; Slane and Thelen, 2015). This may suggest the presence of inter-fascicle sliding and a relative independence of gastrocnemius and soleus tendon components functioning within the Achilles tendon. The fibres of the Achilles tendon may spiral by up to 1.57 rad as they descend towards the attachment site on the calcaneus, with the degree of rotation varying according to the nature and extent of the fusion between gastrocnemius and soleus tendon components within the Achilles tendon (Cummins and Anson, 1946) and also varying considerably between individuals (Bojsen-Moller and Magnusson, 2015). This complex 3D micro-structure will have implications for the degree of deformation occurring along the different regions of the Achilles tendon, probably determining areas of shear and torsional stress concentration. This is reflected by markedly different values for Poisson's ratio between the proximal and distal Achilles tendon regions (Table 3). It might be speculated that rather than differences in tendon CSA as we initially hypothesised, the complex 3D micro-structure and the potential for shear within the tendon could be factors contributing to the high rupture rate of the Achilles tendon 3–5 cm proximal to the calcaneus (Józsa et al., 1989). To determine the effects of different structural distributions

within and along the Achilles tendon, construction of a finite element model is required similar to that previously performed for the patellar tendon (Lavagnino et al., 2008).

The approach followed in the present study involved isometric contractions being held for 2 min duration during MRI scanning. During prolonged constant tensile loading, there is the potential for tendon creep to occur and we therefore tested for this possibility using ultrasound scanning. Our results showed no significant increase in longitudinal tendon elongation during this constant contraction over a 3 min period (i.e. longer than our actual MRI scanning period), indicating that creep was unlikely to be present in our MRI measurements for the range of loading levels examined (Fig. 3). The absence of creep may be explained by the lower level of contractions elicited here (up to 30% MVC) compared with other studies where creep has been observed (Cohen et al., 1976; Maganaris et al., 2002).

Co-activation of dorsiflexor muscles was also unlikely to play any role in our MRI measurements at the range of voluntary forces examined, as the estimated dorsiflexor co-activation torque was <1%. Our participants demonstrated on the dynamometer that they were capable of maintaining the target torque very accurately during plantarflexion contractions with visual feedback at the elicited torque levels (Table 1). We are therefore confident that participants maintained the torque level constant in the MRI scanner during the acquisition of the scans. Additionally, our plantarflexion lever system was very sensitive and the experimenter present in the MRI scanner could identify whether any deviations occurred from the balanced situation.

Certain limitations and assumptions of the current work should be noted. In the present study, we examined plantarflexion contractions up to the level of 30% MVC because of the constraints associated with the length of time contractions needed to be maintained in the MRI scanner (2 min); therefore, caution should be emphasised in extrapolating the current findings to higher forces approaching MVC. Although it might be argued that these force levels (10%, 20% and 30% MVC) are at the relatively low end in relation to MVC forces, the largest elongations occur within the initial low-force region of the tendon force–elongation curve (Butler et al., 1978). In fact, at force levels corresponding to 30% of MVC, tendon elongation is ~50–60% of the elongation measured at 100% of MVC (Malliaris et al., 2013; Reeves et al., 2003, 2005). Hence, by examining tendon deformations at loads up to 30% of MVC, we actually cover a force range accounting for 50–60% of its entire elongation. Because of constraints of the MRI field of view, we were not able to scan the entire length of the proximal part of the Achilles tendon, which should be acknowledged as a limitation. For calculation of the mechanical properties of this proximal part of the tendon, it was therefore necessary to estimate its length using an anthropometric ratio from published data. When estimating the overall elongation of the distal part of the Achilles tendon in calculating mechanical properties, we applied a ratio from published data to the elongation directly measured higher up at the gastrocnemius MTJ. In calculating stiffness of the distal and proximal portions of the Achilles tendon, although the overall force–elongation relationship was curvilinear, a necessary simplification made in the present study (and all previous studies of a similar nature) was to assume linearity of specific but small sections of this force–elongation curve.

In conclusion, using a novel MRI-based approach, the present study shows marked differences along the length of the Achilles tendon, with larger transverse tendon deformations upon tensile loading within the proximal compared with the distal region of the

Achilles tendon. These marked differences were reflected by the force on the proximal tendon region being ~60% lower, stress ~70% lower, stiffness ~30% lower and Poisson's ratio 6-fold higher compared with the distal Achilles tendon component. These results suggest that the proximal component of the Achilles tendon may act as a mechanical buffer to protect the stiffer, more highly stressed, distal component of the Achilles tendon from injury.

Acknowledgements

Many thanks to Diane Chrapkowski for her role in the data collection for this study.

Competing interests

The authors declare no competing or financial interests.

Author contributions

N.D.R. conceived the project idea. N.D.R. and G.C. were both involved in collecting the data for the study. N.D.R. conducted all image analysis. N.D.R. primarily drafted the manuscript with both N.D.R. and G.C. reviewing manuscript drafts and providing final approval.

Funding

This work was supported by funding from the Engineering and Physical Sciences Research Council (EPSRC), via the 'Nano-info-bio' project.

References

- Arampatzis, A., Karamanidis, K. and Albracht, K. (2007). Adaptational responses of the human Achilles tendon by modulation of the applied cyclic strain magnitude. *J. Exp. Biol.* **210**, 2743–2753.
- Arndt, A., Bengtsson, A.-S., Peolsson, M., Thorstensson, A. and Movin, T. (2012). Non-uniform displacement within the Achilles tendon during passive ankle joint motion. *Knee Surg. Sports Traumatol. Arthrosc.* **20**, 1868–1874.
- Bojsen-Moller, J. and Magnusson, S. P. (2015). Heterogeneous loading of the human achilles tendon In Vivo. *Exerc. Sport Sci. Rev.* **43**, 190–197.
- Bojsen-Moller, J., Hansen, P., Aagaard, P., Svantesson, U., Kjaer, M. and Magnusson, S. P. (2004). Differential displacement of the human soleus and medial gastrocnemius aponeuroses during isometric plantar flexor contractions in vivo. *J. Appl. Physiol.* **97**, 1908–1914.
- Butler, D. L., Grood, E. S., Noyes, F. R. and Zernicke, R. F. (1978). Biomechanics of ligaments and tendons. *Exerc. Sport Sci. Rev.* **6**, 125–181.
- Cohen, J. (1988). *Statistical Power Analysis for the Behavioral Sciences*, 2nd edn. Hillsdale, NJ: Lawrence Erlbaum Associates.
- Cohen, R. E., Hooley, C. J. and McCrum, N. G. (1976). Viscoelastic creep of collagenous tissue. *J. Biomech.* **9**, 175–184.
- Couppé, C., Svensson, R. B., Kongsgaard, M., Kovanen, V., Grossset, J.-F., Snorgaard, O., Bencke, J., Larsen, J. O., Bandholm, T., Christensen, T. M. et al. (2016). Human Achilles tendon glycation and function in diabetes. *J. Appl. Physiol.* **120**, 130–137.
- Cuming, W. G., Alexander, R. M. and Jayes, A. S. (1978). Rebound resilience of tendons in the feet of sheep (*Ovis aries*). *J. Exp. Biol.* **74**, 75–81.
- Cummins, E. J. and Anson, B. J. (1946). The structure of the calcaneal tendon (of Achilles) in relation to orthopedic surgery, with additional observations on the plantaris muscle. *Surg. Gynecol. Obstet.* **83**, 107–116.
- Farris, D. J., Trewartha, G., McGuigan, M. P. and Lichtwark, G. A. (2013). Differential strain patterns of the human Achilles tendon determined in vivo with freehand three-dimensional ultrasound imaging. *J. Exp. Biol.* **216**, 594–600.
- Finni, T., Hodgson, J. A., Lai, A. M., Edgerton, V. R. and Sinha, S. (2003). Nonuniform strain of human soleus aponeurosis-tendon complex during submaximal voluntary contractions in vivo. *J. Appl. Physiol.* **95**, 829–837.
- Franz, J. R., Slane, L. C., Rasseke, K. and Thelen, D. G. (2015). Non-uniform in vivo deformations of the human Achilles tendon during walking. *Gait Posture* **41**, 192–197.
- Fukunaga, T., Roy, R. R., Shellock, F. G., Hodgson, J. A., Day, M. K., Lee, P. L., Kwong-Fu, H. and Edgerton, V. R. (1992). Physiological cross-sectional area of human leg muscles based on magnetic resonance imaging. *J. Orthop. Res.* **10**, 928–934.
- Hansen, P., Aagaard, P., Kjaer, M., Larsson, B. and Magnusson, S. P. (2003). Effect of habitual running on human Achilles tendon load-deformation properties and cross-sectional area. *J. Appl. Physiol.* **95**, 2375–2380.
- Iwanuma, S., Akagi, R., Kurihara, T., Ikegawa, S., Kanehisa, H., Fukunaga, T. and Kawakami, Y. (2011). Longitudinal and transverse deformation of human Achilles tendon induced by isometric plantar flexion at different intensities. *J. Appl. Physiol.* **110**, 1615–1621.
- Józsa, L., Kvist, M., Bálint, B. J., Refly, A., Järvinen, M., Lehto, M. and Barzo, M. (1989). The role of recreational sport activity in Achilles tendon rupture. A clinical, pathoanatomical, and sociological study of 292 cases. *Am. J. Sports Med.* **17**, 338–343.

- Karamanidis, K. and Arampatzis, A.** (2006). Mechanical and morphological properties of human quadriceps femoris and triceps surae muscle-tendon unit in relation to aging and running. *J. Biomech.* **39**, 406-417.
- Kongsgaard, M., Nielsen, C. H., Nielsen, C. H., Hegnsvad, S., Hegnsvad, S., Aagaard, P. and Magnusson, S. P.** (2011). Mechanical properties of the human Achilles tendon, in vivo. *Clin. Biomech.* **26**, 772-777.
- Konow, N. and Roberts, T. J.** (2015). The series elastic shock absorber: tendon elasticity modulates energy dissipation by muscle during burst deceleration. *Proc. R. Soc. B Biol. Sci.* **282**, 20142800.
- Konow, N., Azizi, E. and Roberts, T. J.** (2012). Muscle power attenuation by tendon during energy dissipation. *Proc. Biol. Sci.* **279**, 1108-1113.
- Kubo, K., Kanehisa, H. and Fukunaga, T.** (2002). Effect of stretching training on the viscoelastic properties of human tendon structures in vivo. *J. Appl. Physiol.* **92**, 595-601.
- Lavagnino, M., Arnoczky, S. P., Elvin, N. and Dodds, J.** (2008). Patellar tendon strain is increased at the site of the jumper's knee lesion during knee flexion and tendon loading: results and cadaveric testing of a computational model. *Am. J. Sports Med.* **36**, 2110-2118.
- Lersch, C., Grötsch, A., Segesser, B., Koebke, J., Brüggemann, G.-P. and Potthast, W.** (2012). Influence of calcaneus angle and muscle forces on strain distribution in the human Achilles tendon. *Clin. Biomech.* **27**, 955-961.
- Maganaris, C. N. and Paul, J. P.** (1999). In vivo human tendon mechanical properties. *J. Physiol.* **521**, 307-313.
- Maganaris, C. N. and Paul, J. P.** (2000). In vivo human tendinous tissue stretch upon maximum muscle force generation. *J. Biomech.* **33**, 1453-1459.
- Maganaris, C. N. and Paul, J. P.** (2002). Tensile properties of the in vivo human gastrocnemius tendon. *J. Biomech.* **35**, 1639-1646.
- Maganaris, C. N., Baltzopoulos, V. and Sargeant, A. J.** (1998a). Changes in Achilles tendon moment arm from rest to maximum isometric plantarflexion: in vivo observations in man. *J. Physiol.* **510**, 977-985.
- Maganaris, C. N., Baltzopoulos, V. and Sargeant, A. J.** (1998b). Differences in human antagonistic ankle dorsiflexor coactivation between legs; can they explain the moment deficit in the weaker plantarflexor leg? *Exp. Physiol.* **83**, 843-855.
- Maganaris, C. N., Baltzopoulos, V. and Sargeant, A. J.** (2002). Repeated contractions alter the geometry of human skeletal muscle. *J. Appl. Physiol.* **93**, 2089-2094.
- Maganaris, C. N., Reeves, N. D., Rittweger, J., Sargeant, A. J., Jones, D. A., Gerrits, K. and de Haan, A.** (2006). Adaptive response of human tendon to paralysis. *Muscle Nerve* **33**, 85-92.
- Magnusson, S. P. and Kjaer, M.** (2003). Region-specific differences in Achilles tendon cross-sectional area in runners and non-runners. *Eur. J. Appl. Physiol.* **90**, 549-553.
- Magnusson, S. P., Aagaard, P., Dyhre-Poulsen, P. and Kjaer, M.** (2001). Load-displacement properties of the human triceps surae aponeurosis in vivo. *J. Physiol.* **531**, 277-288.
- Magnusson, S. P., Hansen, P., Aagaard, P., Brønd, J., Dyhre-Poulsen, P., Bojsen-Møller, J. and Kjaer, M.** (2003). Differential strain patterns of the human gastrocnemius aponeurosis and free tendon, in vivo. *Acta Physiol. Scand.* **177**, 185-195.
- Malliaras, P., Kamal, B., Nowell, A., Farley, T., Dhamu, H., Simpson, V., Morrissey, D., Langberg, H., Maffulli, N. and Reeves, N. D.** (2013). Patellar tendon adaptation in relation to load-intensity and contraction type. *J. Biomech.* **46**, 1893-1899.
- Masood, T., Bojsen-Møller, J., Kalliokoski, K. K., Kirjavainen, A., Äärmaa, V., Peter Magnusson, S. and Finni, T.** (2014). Differential contributions of ankle plantarflexors during submaximal isometric muscle action: a PET and EMG study. *J. Electromyogr. Kinesiol.* **24**, 367-374.
- Morrison, S. M., Dick, T. J. M. and Wakeling, J. M.** (2015). Structural and mechanical properties of the human Achilles tendon: sex and strength effects. *J. Biomech.* **48**, 3530-3533.
- Reeves, N. D., Maganaris, C. N. and Narici, M. V.** (2003). Effect of strength training on human patella tendon mechanical properties of older individuals. *J. Physiol.* **548**, 971-981.
- Reeves, N. D., Maganaris, C. N., Ferretti, G. and Narici, M. V.** (2005). Influence of 90-day simulated microgravity on human tendon mechanical properties and the effect of resistive countermeasures. *J. Appl. Physiol.* **98**, 2278-2286.
- Rigby, B. J.** (1964). Effect of cyclic extension on the physical properties of tendon collagen and its possible relation to biological ageing of collagen. *Nature* **202**, 1072-1074.
- Roberts, T. J. and Konow, N.** (2013). How tendons buffer energy dissipation by muscle. *Exerc. Sport Sci. Rev.* **41**, 186-193.
- Slane, L. C. and Thelen, D. G.** (2015). Achilles tendon displacement patterns during passive stretch and eccentric loading are altered in middle-aged adults. *Med. Eng. Phys.* **37**, 712-716.
- Wiesinger, H.-P., Kösters, A., Müller, E. and Seynnes, O. R.** (2015). Effects of increased loading on in vivo tendon properties: a systematic review. *Med. Sci. Sports Exerc.* **47**, 1885-1895.
- Williams, L. N., Elder, S. H., Horstemeyer, M. F. and Harbarger, D.** (2008). Variation of diameter distribution, number density, and area fraction of fibrils within five areas of the rabbit patellar tendon. *Ann. Anat.* **190**, 442-451.
- Wren, T. A. L., Yerby, S. A., Beaupré, G. S. and Carter, D. R.** (2001). Mechanical properties of the human achilles tendon. *Clin Biomech* **16**, 245-251.
- Zernicke, R. F., Butler, D. L., Grood, E. S. and Hefzy, M. S.** (1984). Strain topography of human tendon and fascia. *J. Biomech. Eng.* **106**, 177-180.